REPORT DOCUMENTATION PAGE

Form Approved
OMB No. 0704-01-0188

PLEASE DO NOT RETURN YOUR FORM TO THE ABOVE ADDRESS.

1. REPORT DATE *(DD-MM-YYYY)*	2. REPORT TYPE	3. DATES COVERED *(From - To)*
18 May 2007	REPRINT	

4. TITLE AND SUBTITLE

A space-based proxy for the *Dst* index

5a. CONTRACT NUMBER

5b. GRANT NUMBER

5c. PROGRAM ELEMENT NUMBER
61102F

6. AUTHORS

F.J. Rich, J.M. Bono*, W.J. Burke** and L.C. Gentile**

5d. PROJECT NUMBER
2311

5e. TASK NUMBER
SD

5f. WORK UNIT NUMBER
A3

7. PERFORMING ORGANIZATION NAME(S) AND ADDRESS(ES)

Air Force Research Laboratory /VSBXP
29 Randolph Road
Hanscom AFB, MA 01731-3010

8. PERFORMING ORGANIZATION REPORT NUMBER
AFRL-RV-HA-TR-2007-1114

9. SPONSORING/MONITORING AGENCY NAME(S) AND ADDRESS(ES)

10. SPONSOR/MONITOR'S ACRONYM(S)
AFRL/VSBXP

11. SPONSOR/MONITOR'S REPORT NUMBER(S)

12. DISTRIBUTION/AVAILABILITY STATEMENT
Approved for Public Release; distribution unlimited.

13. SUPPLEMENTARY NOTES
Reprinted from *Journal of Geophysical Research*, **112**, A05211, doi:10.1029/2005JA011586 ©2007, American Geophysical Union. *Air Force Inst. of Technology, Wright-Patterson AFB, OH. **Institute for Scientific Research, Boston College, Chestnut Hill, MA 02467.

14. ABSTRACT

The *Dst* index was created to monitor and quantify disturbances in the inner magnetosphere using ground-based, magnetic field measurements. The phases and strengths of geomagnetic storms are usually defined by the evolution of *Dst*. The standard *Dst* database is computed and maintained at the World Data Center for Geomagnetism, Kyoto. We demonstrate that the *Dst* index can also be approximated using magnetometers on spacecraft in near-Earth orbit. Measurements used in the demonstration were obtained from boom-mounted sensors on two spacecraft of the Defense Meteorological Satellite Program. The extraction technique can be applied to magnetic field data retrieved by magnetometers on any spacecraft in low Earth orbit. This alternate method for computing a *Dst*-like index can be used to (1) supplement the standard *Dst* index in near-real-time space weather applications and (2) replace the "prompt" *Dst* index during periods of unavailability.

15. SUBJECT TERMS

Geomagnetic storm
Ring current
Geomagnetic field
Defense Meteorological Satellite Program (DMSP)

16. SECURITY CLASSIFICATION OF:			17. LIMITATION OF ABSTRACT	18. NUMBER OF PAGES	19a. NAME OF RESPONSIBLE PERSON
a. REPORT	b. ABSTRACT	c. THIS PAGE			Frederick J. Rich
UNCL	UNCL	UNCL	UNL		19B. TELEPHONE NUMBER *(Include area code)*

JOURNAL OF GEOPHYSICAL RESEARCH, VOL. 112, A05211, doi:10.1029/2005JA011586, 2007

A space-based proxy for the *Dst* index

F. J. Rich,[1] J. M. Bono,[2,3] W. J. Burke,[1,4] and L. C. Gentile[5]

Received 22 December 2005; revised 18 January 2007; accepted 25 January 2007; published 18 May 2007.

[1] The *Dst* index was created to monitor and quantify disturbances in the inner magnetosphere using ground-based, magnetic field measurements. The phases and strengths of geomagnetic storms are usually defined by the evolution of *Dst*. The standard *Dst* database is computed and maintained at the World Data Center for Geomagnetism, Kyoto. We demonstrate that the *Dst* index can also be approximated using magnetometers on spacecraft in near-Earth orbit. Measurements used in the demonstration were obtained from boom-mounted sensors on two spacecraft of the Defense Meteorological Satellite Program. The extraction technique can be applied to magnetic field data retrieved by magnetometers on any spacecraft in low Earth orbit. This alternate method for computing a *Dst*-like index can be used to (1) supplement the standard *Dst* index in near-real-time space weather applications and (2) replace the "prompt" *Dst* index during intervals of unavailability.

Citation: Rich, F. J., J. M. Bono, W. J. Burke, and L. C. Gentile (2007), A space-based proxy for the *Dst* index, *J. Geophys. Res.*, *112*, A05211, doi:10.1029/2005JA011586.

1. Introduction

[2] The disturbance storm time (*Dst*) index was designed to measure magnetic effects of currents flowing in the equatorial plane of the magnetosphere at approximate distances of several Earth radii (R_E) [*Sugiura*, 1964]. These currents are generated subsequent to plasma injections from the geomagnetic tail into the inner magnetosphere. Since the strengths of plasma injections are regulated by the coupling between the solar wind and the magnetosphere, *Dst* is also a measure of the geoeffectiveness of interplanetary disturbances [*Burton et al.*, 1975].

[3] It is well known that *Dst* is not a perfect indicator of currents in the near-Earth, magnetospheric equatorial plane [*Campbell*, 2004] or of the connection between the interplanetary medium and the magnetosphere [e.g., *O'Brien and McPherron*, 2002; *Cliver et al.*, 2001]. However, *Dst* is widely used in space weather models and is the de facto determinate of whether geomagnetic activity is at quiet, storm, or superstorm levels. While "prompt" versions of this index have generally been available in near-real-time during the past decade, this has not always been true and may not be so in the future. As space weather moves from a pure research topic to a routinely determined set of parameters required for engineering and commercial usage, it seems prudent to investigate alternate methods for estimating the *Dst* index.

[4] This report suggests a new set of procedures for obtaining a parameter that closely tracks the *Dst* index based upon magnetometer measurements from spacecraft of the Defense Meteorological Satellite Program (DMSP) series. While the procedures are not yet fully developed for operational use, the preliminary version reported here shows excellent promise for replicating the *Dst* index.

2. Background

[5] While effects of geomagnetic storms have been observed for a few hundred years, quantitative understanding of their source causes emerged only in the past half-century [*Stern*, 2005]. *Chapman* [1951] suggested that a ring of westward current flows in the equatorial plane during geomagnetic storms to generate southward magnetic field (or negative H component) perturbations at the Earth's surface. The concept of a ring current is now regarded as an over simplified description of the magnetospheric current systems responsible for *Dst*. However, the term continues to be used as a widely accepted metaphor. During storms intensifying electric fields inject plasma from the geomagnetic tail into the inner magnetosphere. Diamagnetic effects and oppositely directed ion and electron gradient-curvature drifts are mainly responsible for causative magnetospheric currents. While some current-carrying particles follow trapped orbits around Earth, many do not. Empirically, the currents associated with stormtime plasma injections are strongest in the midnight to dusk local time (LT) sector.

[6] *Dst* was formulated [*Dessler and Parker*, 1959; *Sugiura*, 1964] as a tool for tracking and quantifying the duration and energy content of the magnetospheric currents. The *Dst* index is compiled from magnetic field records of four, off-equator stations. Secular variations of the main

[1]Space Vehicles Directorate, Air Force Research Laboratory, Hanscom Air Force Base, Massachusetts, USA.
[2]Air Force Institute of Technology, Wright-Patterson Air Force Base, Ohio, USA.
[3]Now at Air Force Weather Agency, Hamilton, Massachusetts, USA.
[4]Also at Institute for Scientific Research, Boston College, Chestnut Hill, Massachusetts, USA.
[5]Institute for Scientific Research, Boston College, Chestnut Hill, Massachusetts, USA.

0148-0227/07/2005JA011586$09.00

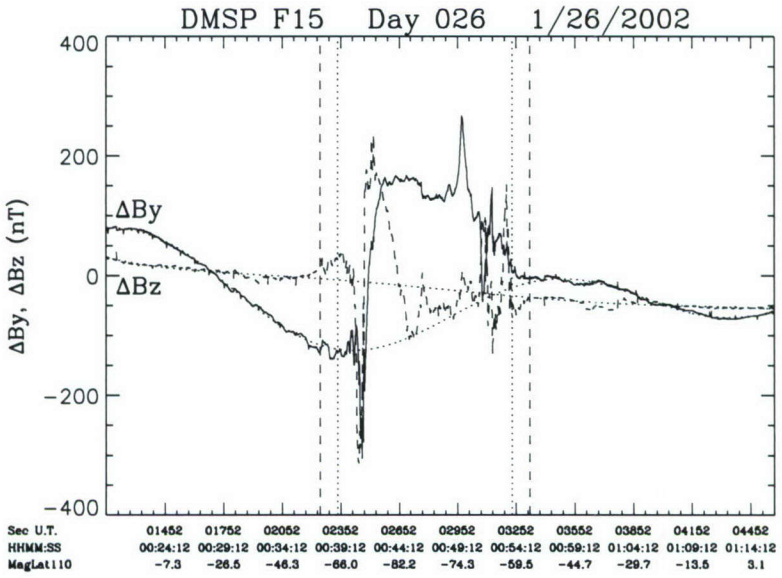

Figure 1. Example of the Defense Meteorological Satellite Program (DMSP) magnetic field vector minus the International Geomagnetic Reference Field (IGRF) magnetic field in the coordinate system of the spacecraft. Only the Y (forward) and Z (cross-track) components are shown. The vertical dotted lines represent the equatorward edges of the auroral electron precipitation zones. The vertical dashed lines represent the limits of the high latitude region excluded from a fit to the data. The dotted curved lines across the figure represent the polynomial fits to the data.

field are first removed from the H-component traces from the four stations. Subsequently seasonally dependent, quiet-day variations are subtracted from the residuals to obtain the disturbance daily variations at each station location. These variations are then divided by cos θ, where θ represents the geomagnetic latitudes of the stations. The perceived need for this "correction" assumes that a simple ring of current flows in the magnetospheric equatorial plane. The average of the remaining four values is the *Dst* index. As it became obvious that magnetospheric currents vary significantly with LT, a corrective term "partial ring current" was added to the geomagnetic vocabulary without changing the definition of *Dst*.

[7] The terms "ring current" and "partial ring current" imply simple sets of currents. Although these terms are convenient and widely used, they describe the configuration of magnetospheric currents inaccurately. Responsible currents are actually temporally and spatially varying ensembles of currents. Modeling by *Tsyganenko and Sitnov* [2005, and references therein] shows that during the main phase of major geomagnetic storms, *Dst* is influenced in decreasing order of importance by the asymmetric (partial) ring current, the near-tail current, the symmetric ring current, and the field-aligned currents (FACs) that couple the magnetosphere to the high-latitude ionosphere and magnetopause currents. During the recovery phase the symmetric ring current is, by far, the dominant contributor.

[8] Geomagnetic storms are driven by disturbed conditions in the interplanetary medium near Earth. The initiation of most storms is marked by a sudden increase in the solar wind's dynamic pressure. Consequent magnetopause-current enhancements cause positive excursions in the H component, known as sudden storm commencements and initial phase. The main phase of a storm occurs while the interplanetary electric field (IEF) has significant dawn-to-dusk components. *Dst* decreases with time, becoming significantly negative with respect to the quiet-time levels. As the IEF's dawn-to-dusk component decays or reverses polarity, the slopes of *Dst*-versus-time traces turn positive and a storm enters its recovery phase. If interplanetary parameters return to sustained predisturbance levels, the *Dst* index approaches quiet-time levels over several days as the symmetric ring current ions are slowly lost via charge exchange with geocoronal neutrals.

[9] *McPherron and O'Brien* [2001] and *Temerin and Li* [2002, 2006] have developed sets of quasi-empirical formulas that compute the evolution of *Dst*, based exclusively on measured interplanetary parameters. While these formulas reproduce the standard *Dst* index quite well, they have not been used in near-real-time operations. The relevant input data for these models are obtained from sensors on research satellites such as the Advanced Composition Explorer near the first Lagrange point. These satellites cannot be relied upon to produce data for years into the future. Also, because the standard *Dst* index has been available on needed timescales, the formulas have not yet found wide usage within the research community.

3. Instrumentation

[10] Spacecraft of the DMSP series fly in polar, circular orbits at ~847 km geocentric altitude with an inclination of 98.8°. This combination forces the orbital plane to precess 360° per year. Thus each spacecraft crosses the equator at approximately the same LT throughout its lifetime. The orbital period of the spacecraft is ~102 min. For DMSP Flight 10 (F10) and beyond, the ascending node is in the

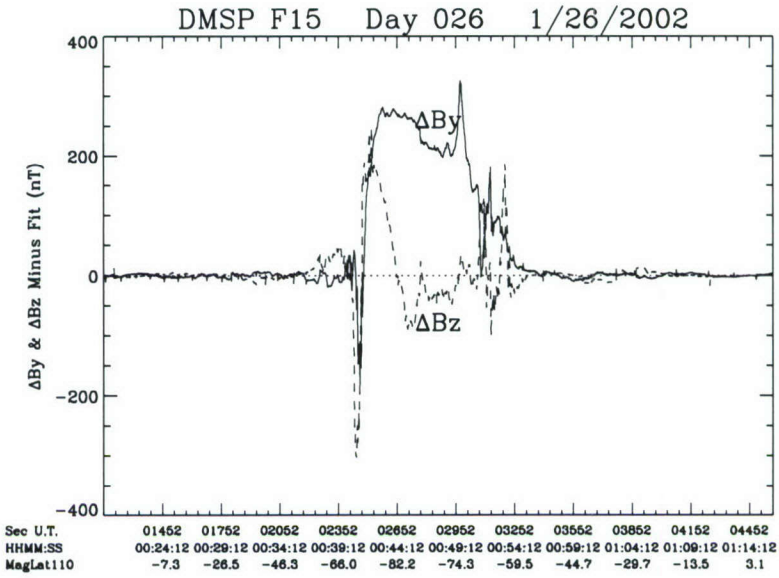

Figure 2. The DMSP magnetic deflection vector after subtracting the fitted polynomial curve from the measured deflection vector shown in Figure 1.

dusk-evening LT sector. Spacecraft attitude is maintained to within 0.01° of the local vertical-forward orientation.

[11] From 1983 to the present, eight DMSP satellites have carried fluxgate (vector) magnetometers. The sensors on F7, F12, F13, and F14 were mounted on the spacecraft frame. Instruments on F12 and beyond are similar to units flown on many NASA missions [*Acuña*, 1974]. DMSP magnetometers measure magnetic field vectors 12 s^{-1} with a resolution of 2 nT in the range of 0 to 4103 nT. They have 64 offsets that extend the range to ±65,660 nT. Sensor mounting has an alignment precision of 0.5° relative to the spacecraft. Postlaunch analysis reduces the alignment precision to between 0.1° and 0.2°. The axes of the sensor and spacecraft align so that X is downward, antiparallel to local vertical, Y is parallel to the spacecraft's velocity vector, and Z is antiparallel to the orbit normal vector. For most uses, including the present work, the measured field is averaged over 1 s and the International Geomagnetic Reference Field (IGRF) is subtracted. Data shown in this paper are differences between measured vectors and those computed using the ninth generation IGRF2000.

[12] Magnetic field sensors were first included on DMSP payloads to identify FACs at high latitudes and to monitor secular variations of the Earth's main field. The goal of identifying FACs has been implemented at the research but not operational level. Owing to excessive noise from the spacecraft the second goal proved unachievable with body-mounted sensors. To reduce noise interference, the magnetic field sensor units were mounted on 5-m booms, starting with F15 (launched in December 1999) and continuing with F16 (October 2003) and F17 (November 2006). Boom-mounting will be provided on all future DMSP spacecraft. The F15 and F16 spacecraft cross the equator at approximately 9 a.m./p.m. and 8 a.m./p.m., respectively. The advent of very high-quality magnetic field instruments on the Ørsted and the Challenging Minisatellite Payload (CHAMP) missions lessened the urgency for using DMSP magnetometer data to model the Earth's main field. Only the cleaner and easier to handle magnetic field data from F15 and F16 are used in this paper.

4. Data Analysis

[13] Our primary goal is to specify deviations of the magnetic-field H component from quiet-time values measured as DMSP spacecraft cross the magnetic equator. This report describes results of newly developed procedures to remove biases and signals, unrelated to geomagnetic activity, from the spacecraft-based Y (forward, horizontal) and Z (cross-track, horizontal) components. We then combine corrected magnetic-field components measured in space to calculate ΔH and compare it with the *Dst* index derived from ground-based data.

[14] In the absence of geomagnetic currents, deflection vectors $\Delta\mathbf{B}$ (= $\mathbf{B}_{measured} - \mathbf{B}_{model}$) should, in principle, be zero. In fact, we usually find nonzero values attributable to uncertainties in sensor alignment and/or calibration, spacecraft-produced magnetic fields and the IGRF model. Figure 1 shows an example of the Y and Z components of $\Delta\mathbf{B}$ acquired during slightly more than half of an orbit of F15. In the present study each analyzed data segment starts a few minutes before a spacecraft crossed the magnetic equator and ends a few minutes after its next equatorial crossing. Data acquired at high magnetic latitudes were excluded to avoid contributions from FACs that electrically couple the ionosphere and magnetosphere. High-latitude segments were designated with reference to equatorward boundaries of auroral electron precipitation, identified in measurements from the SSJ instruments present on all DMSP spacecraft [*Hardy et al.*, 1985]. The auroral electron boundaries are marked by vertical dotted lines in Figure 1. Since the FACs often extend a few degrees in latitude equatorward of auroral electron boundaries, the limits for selecting data are set 90 s (~5°) equatorward. The locations of these subauroral boundaries are marked by vertical dashed lines in Figure 1.

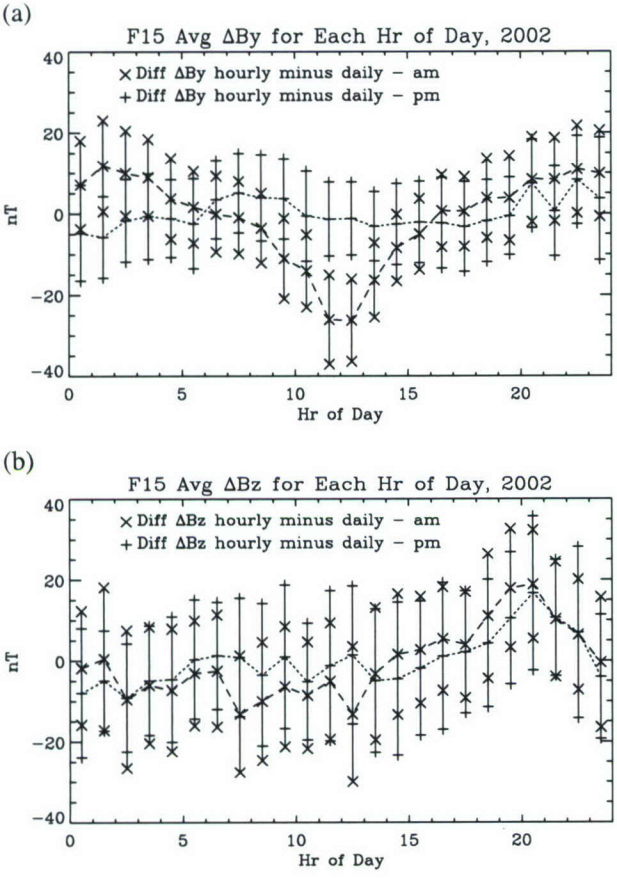

Figure 3. (a) Hourly average of the difference between the Y component of the deflection vector and the daily average as F15 crossed the magnetic equator during 2002. The a.m. (p.m.) averages are connected with a dashed (dotted) line. The differences for the a.m. and p.m. sectors are computed separately. The vertical lines indicate the one-sigma variations of the hourly differences. (b) Same as Figure 3a except the results for the Z component are shown.

[15] At low and middle latitudes, the components of $\Delta\mathbf{B}$ vary more slowly than at high latitudes. However, some variations about uniform trends remain. To determine the trend and exclude small-scale variations, a least squares polynomial was fitted to the data values for each component observed during the ~60 min intervals DMSP satellites spent at subauroral latitudes. Polynomials of order 7 and 5 were applied to ΔB_Y and ΔB_Z measurements, respectively. To insure the goodness of the procedure, we then calculated root-mean-square (rms) differences between the polynomial fits and original data. If the rms for ΔB_Y and ΔB_Z exceeded 15 and 20 nT, respectively, we reset the fitting boundary to 180 s (~10°) equatorward of auroral electron boundaries and repeated the polynomial fitting procedure. If the rms difference still exceeded the specified limits, the particular half-orbit of data was excluded from further processing. Note that our fitting procedure differs significantly from that described by *Higuchi and Ohtani* [2000] for processing DMSP magnetometer data.

[16] Figure 2 shows the result of subtracting fitted polynomials from ΔB_Y and ΔB_Z data. At low and middle latitudes the values are nearly zero. Nonzero values at high latitude are due to the FACs. Developing this procedure was partially motivated by a perceived need to establish baselines for calculating auroral FACs and Poynting vectors during magnetic storms [*Huang and Burke*, 2004].

[17] The present report uses the values of the polynomial fits to ΔB_Y and ΔB_Z at crossings of the magnetic equator along with the LT, date, and time of crossing. Polynomial-fit values are used to suppress small-scale variations due to a variety of factors. At the time of the data in Figure 1, the *Dst* index was near zero. On the basis of geophysical considerations, the DMSP magnetic field deflections ΔB_Y and ΔB_Z should also be near zero. Figure 1 shows they are not zero. However, the observed finite values were found repeatable from orbit to orbit. The present work began after we noticed that DMSP ΔB_Y, the component closest to the direction of **B** at the magnetic equator, varied in time in ways that were strikingly similar to those of *Dst*.

[18] The obvious next step was to subtract constant offsets from the polynomial values of ΔB_Y and ΔB_Z at the magnetic equator. When historic values of *Dst* were near zero, the subtraction of constants appropriate for each component at different spacecraft locations also brought the component values at the magnetic equator to near zero. The constants applicable to the morning and evening sides of the orbit were different and varied from spacecraft to spacecraft but remained consistent from year to year. The constants ranged in absolute value between 20 and 70 nT. Most likely they reflect factors not accounted for in preflight calibrations of the sensors and/or surveys of spacecraft-generated magnetic fields.

[19] We next examined differences between *Dst* and polynomial-fit values for the spacecraft ΔB_Y and ΔB_Z at the magnetic equator crossings as functions of the day of the year. Annual variations exist at the *Dst* stations due to factors such as systematic changes in solar illumination modulating nearby ionospheric currents. Our expectation of identifying similar annual variations in DMSP magnetometer data was not realized. Within an uncertainty of ~10 nT, we found no such variations. At this time, we are unable to explain why a yearly variation was not found.

[20] We also examined differences between *Dst* and the polynomial-fit values at the magnetic equator crossings as a function of the UT hour of the day. A daily variation was expected since the hour of day and longitude are closely linked for Sun-synchronous spacecraft. The geographic latitude of the magnetic equator and the angle between the magnetic and the geographic meridians vary with longitude. Variations at each hour of the day were computed by taking the difference between the polynomial-fit values at each magnetic equator crossing and that day's average of polynomial values at equator crossings. Differences were sorted by universal time. Averages and standard deviations at each hour were computed. If daily averages of ΔB_Y or ΔB_Z plus the bias factor mentioned above were less than −75 nT, the differences for that day were not used in the computation. This minimized the effects of storms on the data. Results for F15 in 2002 appear in Figure 3. The data reveal sufficiently large diurnal variations that must be removed before continuing with the analysis. Within the statistical uncertainty, daily variations for F15 and F16 remained unchanged from year to year.

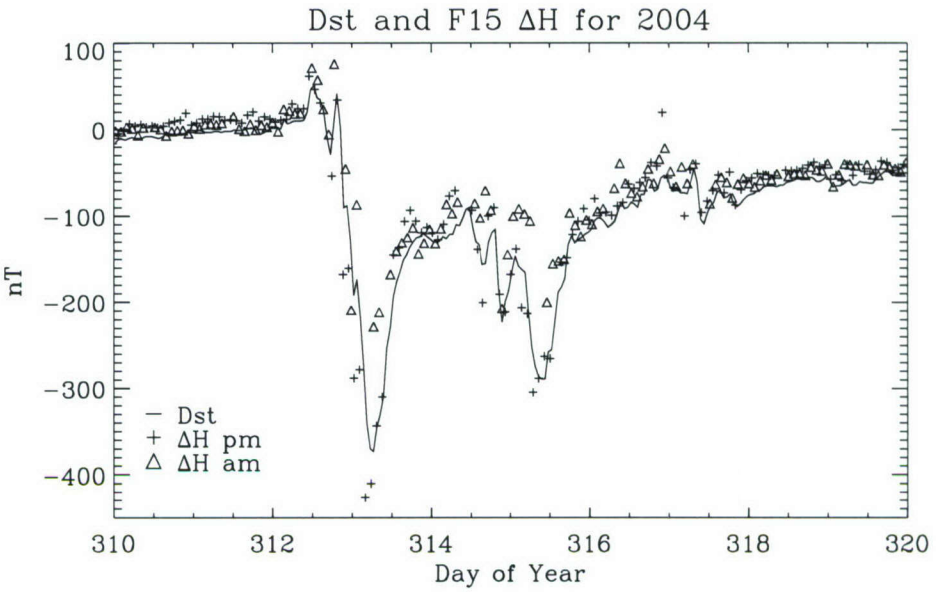

Figure 4. *Dst* index and the ΔH component of the DMSP F15 magnetic field measurement as the a.m. and p.m. magnetic equator are crossed with adjustments as described in the text.

[21] The final step in our analysis was to compute the ΔH component of the magnetic field at DMSP altitude and compare it with the standard *Dst* index. This was done by subtracting the bias values and average hourly variations from each of the ΔB_Y and ΔB_Z values. These deviation components were then added to IGRF field components to create the "effective," measured y and z components ($B'_{Ymeasured}$ and $B'_{Zmeasured}$). The spacecraft-based value for the deviation in the horizontal field is

$$\Delta H = \left(B'^2_{Y\,measured} + B'^2_{Z\,measured}\right)^{1/2} - \left(B^2_{Y\,model} + B^2_{Z\,model}\right)^{1/2} \quad (1)$$

[22] Examples of ΔH derived from DMSP F15 and F16 data are plotted together with the *Dst* index in Figures 4 and 5, respectively. DMSP ΔH values and the *Dst* index are very similar during quiet times. During storms, trends found in DMSP ΔH values appear similar to but not identical with those in the *Dst* trace. ΔH components from the morning and evening sides are plotted separately and differ noticeably during the main phase of storms. We attribute most of this difference to effects of the partial ring current in the evening sector and its absence in the postdawn sector. Magnetic deflections measured at individual *Dst* stations manifest similar evening-morning differences during the main phases of storms. The *Dst* index is computed as the arithmetic average of all *Dst* stations on the assumption that they are adequately distributed in longitude to represent a true globally averaged deflection. Since equatorial sam-

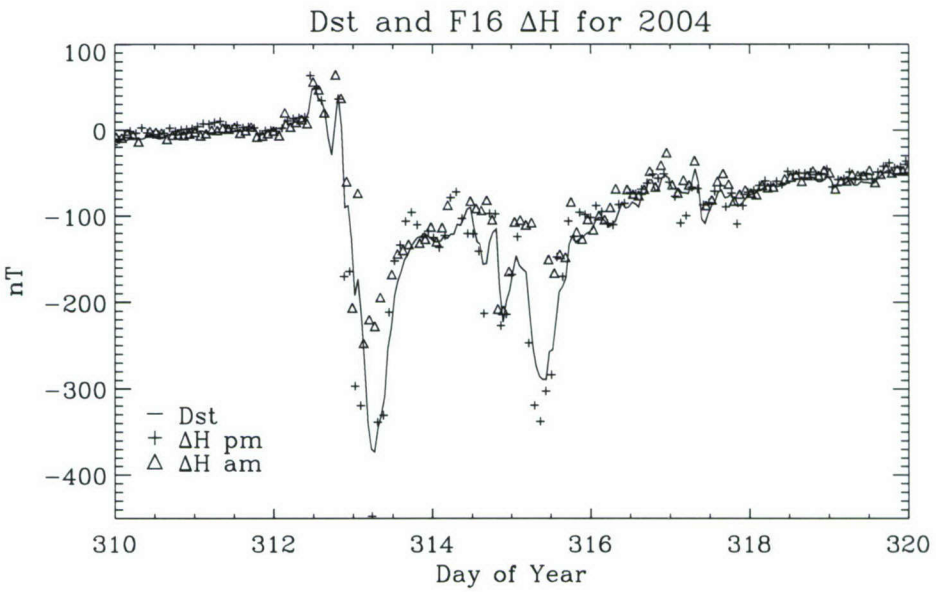

Figure 5. DMSP F16 magnetic field data for the same time period and in the same format as Figure 4.

plings of ΔH by DMSP satellites in the evening and morning sectors are separated by ~50 min in UT, a different averaging scheme must be devised to create a more accurate proxy *Dst* during the main phase of storms.

5. Discussion

5.1. DMSP "*Dst*-Like" Index Versus the Standard *Dst*

[23] Our technique for obtaining a DMSP "*Dst*-like" index has some similarities to those used to convert ground-based magnetic field measurements into the standard *Dst* index. Both data sets have systematic corrections that must be applied to the initial measurements. Both methods of analysis seek to estimate the perturbations at the geomagnetic equator due to magnetospheric current sources. While currents near the magnetospheric, equatorial plane significantly affect ground-based magnetometer measurements, currents in the ionosphere and lithosphere also contribute. In particular, the equatorial electrojet affects ground-based magnetometer readings within 10° to 15° of the magnetic equator. The *Dst* stations are chosen to be at latitudes of 20° to 30° to mitigate perturbations attributable to the electrojet. That decision required the introduction of a correction to account for latitudinal separations between the stations and the magnetic equator. The assumed correction factor may not be appropriate for sets of currents that are spatially and temporally distributed in the inner magnetosphere. Our spacecraft-based measurements are made at the actual magnetic equator and thus do not need this correction factor.

[24] Since DMSP spacecraft fly at ~847 km they should detect stronger perturbations due to magnetospheric currents than are observed at ground level. Assuming that the ring current's centroid is located in the equatorial plane at a radial distance of 5 R_E and can be treated locally as a line current, magnetic deflections at the DMSP altitude should be ~3% larger than on the ground. While differences of this magnitude are not yet obvious in the present level of analysis, systematic, and significant differences may emerge during future studies.

[25] Many users of the standard *Dst* index assume that it is always available and is reasonably accurate in near real time. However, the standard "prompt" *Dst* index was unavailable from early October 2005 to early February 2006. While the "prompt" *Dst* index resumed on an hourly basis and the missing values were provided, no backup index existed during the outage period. In the future, a spacecraft-based index could provide such a backup.

[26] We compared our DMSP-based index against the restored "prompt" *Dst* for October to December 2005. The "prompt" *Dst* values were more negative than the spacecraft proxy. This may reflect an error in "prompt" *Dst* values that was corrected later when the "preliminary" *Dst* was released. Users should always be aware that the World Data Center for Geomagnetism does not promise that the values made available on a "prompt" or near-real-time basis are accurate. Rather it provides *Dst* values on three accuracy levels: "prompt" values are produced within minutes of real time, "preliminary" values become available ~6–9 months after acquisition, and the production of "final" values requires 2 years or more. While some users can afford to wait for the "final" *Dst*, many others must rely on "prompt" values. A second source might help such users weigh uncertainties in corresponding "prompt" *Dst* values.

5.2. DMSP Measurements During Geomagnetic Storms

[27] As shown in Figures 4 and 5, the DMSP index matches *Dst* quite well in quiet and slightly disturbed periods but not during magnetic storms. We analyzed data from the main and early recovery phases of all geomagnetic storms during the 2002–2005 interval. The survey showed that (1) DMSP ΔH values obtained in the morning sector were less negative than both *Dst* and values measured on the eveningside, (2) ΔH obtained in the evening sector was more negative than *Dst*, and (3) after the recovery phase was underway for 2–4 hours, morning and evening DMSP ΔH values converged with each other and *Dst*. The morning/evening difference reflects the asymmetry of the magnetospheric current system during the main phase of storms when large quantities of plasma were energized and injected into the inner magnetosphere.

[28] Most storm-injected ions drift westward across the evening-afternoon sector of the inner magnetosphere. Some energetic ions become trapped on closed paths around the Earth. Conversely, most energetic electrons drift eastward across the morning sector. The pressure of the ring-current ions (P_i) exceeds that of the electrons (P_e). Force balance requires that the current density ($j_\perp$) perpendicular to the local magnetic field B is

$$\vec{j}_\perp = -\frac{\nabla(P_i + P_e) \times \vec{B}}{B^2} \tag{2}$$

With the strongest pressure gradients developing in the midnight-dusk sector, we expect that magnetic perturbations at the Earth's surface, produced by ring current particles, should be stronger at these local times. After injection drivers diminish or stop, some particles continue to drift out of the magnetosphere while the rest become confined to trapped orbits. Thus the recovery phase ring current evolves toward the symmetric, near-equatorial configuration initially suggested by *Chapman* [1951]. Observed differences between the DMSP ΔH measured in the dusk and dawn sectors may offer advantages. DMSP data, in coordination with other space- and ground-based measurements can be used to improve models of the asymmetric ring current's birth-death cycle.

6. Conclusions

[29] This paper demonstrates substantial agreement between our DMSP ΔH and the standard *Dst* index. With further development, a DMSP index could provide an alternate method of computing *Dst* for use in space weather models. The major advantage is that the DMSP data are rapidly available within the operational space weather community and the DMSP index can be derived with much less human involvement. In addition, the DMSP magnetometers are space assets whose availability is guaranteed for the next decade. The major disadvantage is that the index can only be updated at intervals of several minutes as various contributing spacecraft cross the magnetic equator. Ground-based magnetic field data are updated at 1-min

intervals. This disadvantage can be reduced by the inclusion of magnetic field data from other satellites in low-Earth-orbit. In particular, if data from the Iridium series of spacecraft [*Anderson et al.*, 2002] were added, the space-based index could be updated every 5 min. Currently, the resolution of data sampled by Iridium magnetometers is inadequate for computing a *Dst*-like index. However, this deficiency can and may well be remedied in the near future.

[30] **Acknowledgments.** The work of J. Bono was done in partial fulfillment of the requirements for a Master of Science degree. We wish to thank his thesis advisor Devin Della-Rose, formally at AFIT and now at the U.S. Air Force Academy. This work was also supported at AFRL under AFOSR Task 2311SDA3 and Air Force contract F19628-02-C-0012 with Boston College. We wish to thank Ethan Sexton of Radex Inc., who helped with the first version of this work. *Dst* values were obtained from the World Data Center, Kyoto (http://wdcwww.kugi.kyoto-u.ac.jp).

[31] Zuyin Pu thanks Wallace Campbell and another reviewer for their assistance in evaluating this paper.

References

Acuña, M. (1974), Fluxgate magnetometer for outer planetary exploration, *IEEE Trans. Magn., 10*, 3, 519–523.

Anderson, B. J., K. Takahashi, T. Kamei, C. L. Waters, and B. A. Toth (2002), Birkeland current system key parameters derived from Iridium observations: Method and initial validation results, *J. Geophys. Res.*, *107*(A6), 1079, doi:10.1029/2001JA000080.

Burton, R. K. J., R. L. McPherron, and C. T. Russell (1975), An empirical relationship between interplanetary conditions and *Dst*, *J. Geophys. Res.*, *80*, 4204–4214.

Campbell, W. H. (2004), Failure of *Dst* index fields to represent a ring current, *Space Weather*, *2*, S08002, doi:10.1029/2003SW000041.

Chapman, S. (1951), *The Earth's Magnetism*, 127 pp., John Wiley, Hoboken, N. J.

Cliver, E. W., Y. Kamide, A. G. Ling, and N. Yokoyama (2001), Semiannual variation of the geomagnetic *Dst* index: Evidence for a dominant nonstorm component, *J. Geophys. Res.*, *106*, 21,297–21,304.

Dessler, A. J., and E. N. Parker (1959), Hydromagnetic theory of magnetic storms, *J. Geophys. Res.*, *64*, 2239–2259.

Hardy, D. A., M. S. Gussenhoven, and E. Holeman (1985), A statistical model of auroral electron precipitation, *J. Geophys. Res.*, *90*, 4229–4248.

Higuchi, T., and S. Ohtani (2000), Automatic identification of large-scale field-aligned current structures, *J. Geophys. Res.*, *105*, 25,305–25,315.

Huang, C. Y., and W. J. Burke (2004), Transient sheets of field-aligned current observed by DMSP during the main phase of a magnetic storm, *J. Geophys. Res.*, *109*, A06303, doi:10.1029/2003JA010067.

McPherron, R. L., and T. P. O'Brien (2001), Predicting geomagnetic activity: The *Dst* index, in *Space Weather*, *Geophys. Monogr. Ser.*, vol. 155, edited by P. Song, G. L. Siscoe, and H. Singer, pp. 339–345, AGU, Washington, D. C.

O'Brien, T. P., and R. L. McPherron (2002), Seasonal and diurnal variations of *Dst* dynamics, *J. Geophys. Res.*, *107*(A11), 1341, doi:10.1029/2002JA009435.

Stern, D. P. (2005), A historical introduction to the ring current, in *The Inner Magnetosphere: Physics and Modeling*, *Geophys. Monogr. Ser.*, vol. 155, edited by T. I. Pulkkinen, N. A. Tsyganenko, and R. H. W. Friedel, pp. 1–8, AGU, Washington, D. C.

Sugiura, M. (1964), Hourly values of the equatorial *Dst* for the IGY, *Ann. Int. Geophys. Year*, *35*, 9.

Temerin, M., and X. Li (2002), A new model for the prediction of *Dst* on the basis of the solar wind, *J. Geophys. Res.*, *107*(A12), 1472, doi:10.1029/2001JA007532.

Temerin, M., and X. Li (2006), *Dst* model for 1995–2002, *J. Geophys. Res.*, *111*, A04221, doi:10.1029/2005JA011257.

Tsyganenko, N. A., and M. I. Sitnov (2005), Modeling the dynamics of the inner magnetosphere during strong geomagnetic storms, *J. Geophys. Res.*, *110*, A03208, doi:10.1029/2004JA010798.

J. M. Bono, Air Force Weather Agency, Det. 2, Sagamore Hill Solar Observatory, Hamilton, MA 01983, USA. (james.bono@hanscom.af.mil)

W. J. Burke and F. J. Rich, Space Vehicles Directorate, Air Force Research Laboratory, Hanscom AFB, MA 01731, USA. (william.burke2@hanscom.af.mil; frederick.rich@hanscom.af.mil)

L. C. Gentile, Institute for Scientific Research, Boston College, Chestnut Hill, MA 02467-3862, USA. (louise.gentile@hanscom.af.mil)